International Journal of Research in Advent Technology, Vol.6, No.11, November 2018
E-ISSN: 2321-9637
Available online at www.ijrat.org

Entropy generation analysis of peristaltic flow of Jeffrey nanofluid in a tube with permeable walls

Tahmeena Kawkab[1],Y.V.K.Ravi Kumar[2],C.Uma Devi[3]
[1]*Researsch scholar, Dept. of Mathematics, Rayala Seema University, Kurnool, A.P, India.*
[2]*Asst Prof, Dept. of Mathematics, BITS Pilani, Hyderabad Center, Hyderabad, Telangana, India.*
[3]*Asst Prof, Dept. of Mathematics, TKR CET, Hyderabad, Telangana, India.*
tahmeenakawkab1@gmail.com[1],yvkravi@gmail.com[2],uma140276@gmail.com[3]

Abstract- In the present paper , Entropy generation analysis of peristaltic flow of Jeffery nanofluid in a tube with permeable walls has been studied. Mathematical modelling of the governing fluid flow problem is formulated and solved under the longwave length low Reynold number assumptions. The analytical solution of Velocity and temperature distribution are obtained. It can be Observed from the graphs that entropy generation attains maximum value near the walls of the tube and minimum value at the center of the tube.

Keywords- Entropy generation,Jeffery nanofluid,Permeable walls,Peristalsis.

1.INTRODUCTION

Peristalsis is the process of contraction and relaxation of muscle tissue which can allow movement of a substance in a given direction. Study of peristaltic transport captured the interest of many researchers, since it is the one of the basic physiological phenomena which has enormous applications in physiology, ecology, engineering and industry. Some of the basic applications of peristaltic transport are swallowing of food through esophagus, urine transport from kidney to bladder, chime movement in the intestine, movement of eggs in the fallopian tube, transport of cilia, circulation of blood in small vessels, finger and roller pumps for pumping corrosive materials to prevent direct contact of the fluid with the pumps internal surface, toxic liquid transportation in the nuclear industry etc.

Latham[1] is the one who has started experimental study on peristaltic transport in which he studied the fluid motion in a peristaltic pump. His research inspired many to do reseach in the related areas. Shapiro et al.[2] proposed a descriptive analysis of peristaltic flow of Newtonian fluid, in which he has considered long wave length and low Reynold number. Srinivasa and Kothandapani [3] discussed the peristaltic transport of viscous fluid in an asymmetric channel. Later extensive research has been done on peristaltic transport of different fluid models under different conditions (Akber et al. [4], Mekhemier[5], Devi and Devanathan [6], Muthu et al.[7]).

Choi[8] proposed the name Nanofluid, which is defined as a convectional heat transfer base fluid with mixture of ultrafine nanosized particles. The physical and chemical characteristics of these particles are different. The nanoparticles have high thermal conductivity comparative to the base fluids. In recent years, the study of nanofluid has gained its popularity due to its extensive applications in bio and mechanical industries such as paper, printing, paints and cancer therapy etc. In view of this, the contributions of peristaltic transport of nanofluids have been studied [9,10,11] .

Jeffrey fluid is a non-Newtonian fluid, which describes the characteristics of retardation and relaxation times. This model is one of the simplest but most used model because of this feature. Akbar and Nadeem [12] studied the mixed convective peristaltic motion of MHD Jeffrey nanofluid in an asymmetric channel with Newtonian heating. A theoretical investigation on Peristaltic transport of effrey nanofluid in curved channel was analyzed by Narla et al.[13].

Entropy is defined as the measure of irreversibility or degree of disorder associated with heat transfer processes. Li and Kleinstreuer [14] analyzed the entropy generation in trapezoidal micro channels for pure water and Cuo- water nanofluids. The rate of entropy generation for a peristaltic pump was studied by Souidi et al.[15]. Hayat et al.[16] examined the entropy generation analysis on peristaltic transport of nanofluid in a tube with flexible walls. Akbar and Butt [17] studied the analysis of entropy generation

for the peristaltic flow of Cu-water nanofluid in a channel by considering viscous dissipation.

2. PROBLEM FORMULATION

Consider the incompressible peristaltic flow of Jeffrey nanofluid in a horizontal tube with permeable walls. A sinusoidal wave is disseminating through the walls of the tube. Cylindrical polar coordinate system (R, Z) is chosen. Here Z- axis is taken as the horizontal axis, which coincides with the center of tube and R is the vertical axis. Further, the flow is assumed to be symmetric. The wave is propagated with a velocity C along the wall of the tube.

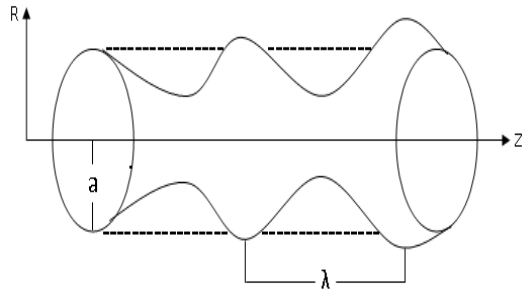

Fig. 1 Geometry of the Problem

The geometry of the wall surface is given as

$$H = a + b\,Sin\frac{2\pi}{\lambda(Z - Ct)} \qquad \text{Eq. (1)}$$

Where a is the radius of the tube, b is the sinusoidal wave amplitude, C is the wave speed and λ is the wavelength, t is the time.

The geometry of the flow is exhibited in the figure 1

The relations between fixed frame and wave frame are given as

$\bar{r}$=R, $\bar{z}$=Z-Ct, $\bar{u}$=U, $\bar{w}$=W-C Eq. (2)

The governing equations and the boundary conditions for the flow of an incompressible Jeffrey nanofluid are

$$\frac{1}{\bar{r}}\frac{\partial(\bar{r}\bar{u})}{\partial\bar{r}} + \frac{\partial(\bar{w})}{\partial\bar{z}} = 0 \qquad \text{Eq. (3)}$$

$$\rho_{Nf}\left((\bar{u})\frac{\partial(\bar{u})}{\partial\bar{r}} + (\bar{w})\frac{\partial(\bar{w})}{\partial\bar{z}}\right) = -\frac{\partial\bar{p}}{\partial\bar{r}} + \frac{1}{\bar{r}}\frac{\partial}{\partial\bar{r}}(\bar{r}S_{\bar{r}\bar{r}}) + \frac{\partial}{\partial\bar{z}}(S_{\bar{r}\bar{z}}) \qquad \text{Eq. (4)}$$

$$\rho_{Nf}\left((\bar{u})\frac{\partial(\bar{w})}{\partial\bar{r}} + (\bar{w})\frac{\partial(\bar{w})}{\partial\bar{z}}\right) = -\frac{\partial\bar{p}}{\partial\bar{z}} + \frac{1}{\bar{r}}\frac{\partial}{\partial\bar{r}}(\bar{r}S_{\bar{r}\bar{z}}) + \frac{\partial}{\partial\bar{z}}(S_{\bar{z}\bar{z}}) - \sigma B_0^2(\bar{w} + c) \qquad \text{Eq. (5)}$$

$$\frac{\partial(\bar{u})}{\partial\bar{r}} + \frac{\partial(\bar{w})}{\square}/ \qquad \text{Eq. (6)}$$

The stress tensor components are

$$S_{\bar{r}\bar{r}} = \frac{2\mu}{1+\lambda_1}\left(1 + \lambda_2\left(\frac{\bar{w}\partial}{\partial\bar{r}} + \frac{\bar{u}\partial}{\partial\bar{z}}\right)\frac{\partial\bar{w}}{\partial\bar{r}}\right)$$

$$S_{\bar{r}\bar{z}} = \frac{\mu}{1+\lambda_1}\left(1 + \lambda_2\left(\frac{\bar{w}\partial}{\partial\bar{r}} + \frac{\bar{u}\partial}{\partial\bar{z}}\right)\right)\left(\frac{\partial\bar{u}}{\partial\bar{r}} + \frac{\partial\bar{w}}{\partial\bar{z}}\right)$$

$$S_{\bar{z}\bar{z}} = \frac{2\mu}{1+\lambda_1}\left(1 + \lambda_2\left(\frac{\bar{w}\partial}{\partial\bar{r}} + \frac{\bar{u}\partial}{\partial\bar{z}}\right)\frac{\partial\bar{u}}{\partial\bar{r}}\right)$$

Where $\bar{u}, \bar{w}$ are the velocity components in in the directions of $\bar{r}$ and $\bar{z}$ respectively. $\bar{T}$ is the local temperature of the fluid, μ_{Nf} is dynamic viscosity, ρ_{Nf} is effective density, $(\rho_{cp})_{Nf}$ is heat capacitance, k_{Nf} is effective thermal conductivity and $\bar{p}$ is pressure.

The non-dimensional variables are

$$r = \frac{\bar{r}}{A}, z = \frac{\bar{z}}{\lambda}, w = \frac{\bar{w}}{C}, u = \frac{\lambda\bar{u}}{AC}, p = \frac{A^2\bar{p}}{C\lambda\mu_f}, \delta = \frac{A}{\lambda}, \theta = \frac{\bar{T} - \bar{T}_0}{\bar{T}_0}, M^2 = \frac{\sigma B_0^2 A^2}{\mu_f}, B_r = E_c P_r \qquad \text{Eq. (7)}$$

Making use of these variables, in Eqs.(3) to (6) under the assumptions of long wave length and low Reynolds number approximation we get the reduced equations are as follows

$$\frac{dp}{dr} = 0 \qquad \text{Eq. (8)}$$

$$\frac{\partial p}{\partial z} = \left(\frac{\mu_{nf}}{\mu_f}\right)\frac{1}{r}\frac{\partial}{\partial r}\left(\frac{r}{1+\lambda_1}\frac{\partial w}{\partial r}\right) - M^2(w+1) \qquad \text{Eq. (9)}$$

$$\left(\frac{k_{nf}}{k_f}\right)\frac{1}{r}\frac{\partial}{\partial r}\left(\frac{r}{1+\lambda_1}\frac{\partial\theta}{\partial r}\right) + B_r\left(\frac{\mu_{nf}}{\mu_f}\right)\left(\frac{\partial w}{\partial r}\right)^2 = 0 \qquad \text{Eq. (10)}$$

The non-dimensional boundary conditions are

$$\frac{\partial w}{\partial r} = 0, \frac{\partial \theta}{\partial r} = 0 \ at \ r = \mathbf{0} \qquad \text{Eq. (11)}$$

$$w + \beta \frac{\partial w}{\partial r} = 0, \theta + \gamma \frac{\partial \theta}{\partial r} = 0 \ at \ r = \boldsymbol{h} \qquad \text{Eq. (12)}$$

Where $\beta = \frac{\sqrt{D_a}}{\alpha}$, D_a is Darcy number, α slip parameter

Thermal properties of the fluid are given as follows [references (18-20)]

$$\rho_{nf} = (\mathbf{1} - \varphi)\rho_f + \varphi\rho_f, \mu_{nf} = \frac{\mu_f}{(\mathbf{1} - \varphi)^{2.5}},$$

$$(\rho c_p)_{nf} = (\mathbf{1} - \varphi)([\rho c_p)]_f + \varphi(\rho c_p)_s,$$

$$\alpha_{nf} = \frac{k_{nf}}{(\rho c_p)_{nf}}, k_{nf} = k_f \left[\frac{k_s + 2k_f - 2\varphi(k_f - k_s)}{k_s + 2k_f + 2\varphi(k_f - k_s)}\right]$$

Where M is Hartman number, B_r is Brinkman number, P_r is Prandtl number and φ is the nanoparticle volume fraction.

2.1 Entropy Generation Analysis

Souidi et al. [15] defined Entropy generation as

$$S_G = \frac{K_{Nf}}{\bar{T}_0}\left[\left(\frac{\partial \bar{T}}{\partial \bar{r}}\right)^2 + \left(\frac{\partial \bar{T}}{\partial \bar{z}}\right)^2\right] + \mu_{Nf}\left\{2\left[\left(\frac{\partial \bar{u}}{\partial \bar{z}}\right)^2 + \left(\frac{\partial \bar{w}}{\partial \bar{r}}\right)^2\right] + \left(\frac{\partial \bar{u}}{\partial \bar{z}} + \frac{\partial \bar{w}}{\partial \bar{r}}\right)^2\right\} + \frac{\sigma B_0^2}{\bar{T}_0}(\bar{w} + c) \qquad \text{Eq. (13)}$$

Dimensionless form of Entropy Generation is given as

$$N_S = \frac{S_G}{S_{G_0}} = \left(\frac{K_{Nf}}{K_f}\right)\left(\frac{\partial \theta}{\partial r}\right)^2 + \frac{B_r}{\Lambda}\left(\frac{\mu_{Nf}}{\mu_f}\right)\left(\frac{\partial w}{\partial r}\right)^2 + \frac{M^2 B_r}{\Lambda}(w + 1)^2 \qquad \text{Eq. (14)}$$

Where S_G is the entropy generation rate, S_{G_0} is characteristic entropy transfer rate

$$S_{G_0} = \frac{K_{Nf}\Delta\bar{T}}{\bar{T}_0 a^2}, \Lambda = \frac{\Delta\bar{T}}{\bar{T}_0} \qquad \text{Eq. (15)}$$

The total entropy generation from equation (14) can be written as the sum

$$N_S = N_H + N_F + N_M = N_H + N_B \qquad \text{Eq (16)}$$

Where N_H is the entropy generation due to heat transfer, N_F is the local entropy generation due to fluid friction irreversibility and N_M is the entropy generation due to magnetic field. Sum of N_F, N_M is considered as entropy generation N_B due to the combined effect of fluid friction and magnetic field.

since $N_S = N_H + N_B$ in order to observe the nature of N_H, N_B the irreversibility ratio is studied, which is the ratio between entropy generation due to fluid friction and joule dissipation to the total entropy generation due to heat transfer.

Irreversibility ratio $\bar{\xi}$ is defined as the ratio of fluid friction irreversibility to the irreversibility due to heat transfer.

$$\bar{\xi} = \frac{N_B}{N_H} = \frac{\frac{B_r}{\Lambda}\left(\frac{\mu_{Nf}}{\mu_f}\right)\left(\frac{\partial w}{\partial r}\right)^2 + \frac{M^2 B_r}{\Lambda}(w + 1)^2}{\left(\frac{K_{Nf}}{K_f}\right)\left(\frac{\partial \theta}{\partial r}\right)^2} \qquad \text{Eq. (17)}$$

Irreversibility ratio $\bar{\xi}$ dominates in the interval $(0,1)$ and when $\bar{\xi} > 1$ shows that Irreversibility is due to heat transfer. Fluid friction and heat transfer have same effect when $\bar{\xi} = 1$.

Bejan number is also an Irreversibility parameter

defined as

$$B_e = \frac{N_B}{N_H} = \frac{1}{1 + \bar{\xi}} \qquad \text{Eq. (18)}$$

3. Solution of the problem

Solving Eqs. (9) and (10) together with the boundary conditions, we get the solution for the velocity of the fluid as follows

$$w(r,z)=\frac{\left[\frac{1}{M^2}\left(\frac{\partial p}{\partial z}\right)+1\right]I_0\left(Mr\sqrt{(1+\lambda_1)(1-\varphi)^{2.5}}\right)}{I_0\left(Mh\sqrt{(1+\lambda_1)(1-\varphi)^{2.5}}\right)+\beta\left[M\sqrt{(1+\lambda_1)(1-\varphi)^{2.5}}\,I_1\left(Mh\sqrt{(1+\lambda_1)(1-\varphi)^{2.5}}\right)\right]}-\frac{1}{M^2}\left(\frac{\partial p}{\partial z}\right)-1$$

Eq. (19)

The temperature distribution is given as

$\mathbf{M}^2h^2$ Eq. (20)

Where

$$\varsigma=(1+\lambda_1)\frac{k_f}{k_{nf}}\frac{B_r}{\Lambda}\left[\frac{\left(\frac{1}{M^2}\left(\frac{\partial p}{\partial z}\right)+1\right)M\Theta}{I_0(Mh\Theta)+\beta M\Theta\, I_1(Mh\Theta)}\right]^2,$$

$$\frac{\mu_f}{\mu_{nf}}=(1-\varphi)^{2.5}=$$ Λ and $\Theta=\sqrt{(1+\lambda_1)\Lambda}$

The flow rate is given by

$$F=2\pi\int_0^h rw\,dr$$

$$F=\frac{2\pi\left[\frac{1}{M^2}\left(\frac{dp}{dz}\right)+1\right]}{I_0(Mh\Theta)+\beta\mathbf{M\Theta}\,I_1(Mh\mathbf{\Theta})}\frac{h\,I_1(Mh\mathbf{\Theta})}{M\mathbf{\Theta}}-\frac{2\pi}{M^2}\left(\frac{dp}{dz}\right)\frac{h^2}{2}-\pi h^2$$

Eq. (21)

Then

$$\left(\frac{dp}{dz}\right)=\frac{F+\pi h^2-\frac{2\pi h\, I_1(Mh\Theta)}{M\Theta\{I_0(Mh\Theta)+\beta\mathbf{M\Theta}\,I_1(Mh\mathbf{\Theta})@]}}{\frac{\pi h^2}{M^2}+\frac{2\pi h}{M^3}\frac{I_1(Mh\Theta)}{\mathbf{\Theta}\{I_0(Mh\mathbf{\Theta})+\mathbf{\beta M\Theta}\,I_1(Mh\mathbf{\Theta})\}}}$$

Eq. (22)

Where the mean flow rate Q is given as

$$Q=F+\frac{1}{2}\left(1+\frac{\varepsilon^2}{2}\right)$$ Eq. (23)

Integrating equation (22) in the interval [0,1] pressure rise is obtained as

$$\Delta p=\int_0^1\frac{dp}{dz}dz$$ Eq. (24)

4.Results and Discussions

Through the grahical representation, the influence of various parameters such as velocity(w), pressure gradient($\frac{dp}{dz}$), temperature(θ), entropyanaysis(NS), variation of Bejan number (B_e) etc. are analyzed.

4.1 Velocity profile:

Figure2 represents the variation of velocity (w) of the fuid inside the tube which is plotted against the radial distance (r).This graph depicts the impact of Λ on velocity. The velocity decreases with increasing values of Λ (velocity is maximum at the center and minimum at the walls). The variation of velocity (w) with respect to the variation of Darcy number ($\sqrt{(D_a)}$) is shown in figure 3. It has been observed that the velocity decreases with the decrease in darcy number $\sqrt{(D_a)}$. From figure 4 it is noticed that the slip parameter (α) is inversely proportional to velocity profile (w) .Figure 5 shows the relationship between velocity (w) and hartmann number (M), Velocity gradually decreases with increase in hartmann number(M).It has been observed from figure 6 that velocity increase with increase in the value of ϵ.Figure 7 represents the effect of λ_1 on velocity (w).it can be observed that as the value of λ_1 increases there is a little reduction in the value of velocity(w). We can conclude from the graphs (2-7) that the velocity(w) is maximum at the center and minimum at the walls of the tube.

4.2 Pressure Gradient ($\frac{dp}{dz}$)

Graphs (8-13) shows the impact of various parameters on pressure gradient ($\frac{dp}{dz}$).pressure gradient decreases with increase in Hartmann number (M) in the interval $0\le z\le 0.8$ and it is minimum at 0.8 and then increases from there till the end of the wall. overall it has nonuniform behavior (fig 8). The oscillatory behavior of pressure gradient with the effect of the parameters $\sqrt{(Da)}$ and Δ(fig 9&10).Figure 11 representS the variation of pressure gradient with ϵ .It is interesting to observe that ($\frac{dp}{dz}$) decreases with increase in ϵ in the interval $0\le z\le 0.2$ and the pressure gradient increases with decrease in ϵ in $0.2\le z\le 0.5$ and thereafter pressure gradient is directly proportional to ϵ in the interval $0.5\le z\le 0.7$ and inversely proportional in the interval $0.7\le z\le 1.0$.

Figure 12&13 shows the variation of pressure gradient($\frac{dp}{dz}$) with the parameters Λ and Jeffery fluid parameter (λ_1). It is noted that ($\frac{dp}{dz}$) decreases with increase in Λ and λ_1 in the interval $0 \le z \le 0.2$ and increases in the interval $0.2 \le z \le 0.7$ and decreases thereafter,it is observed from the graph that ($\frac{dp}{dz}$) is minimum at $z = 0.2$ and maximum at $z = 0.7$.

Figure 14 &15 reflects the influence of Bronian motion number (B_r), Hartmann number (M) on temperature θ. Temperature of fluid in the tube decreases with increase in Bronian motion number and Hartmann number. Temprature is maximum at center r$= 0$ and minimum at the walls of the tube.

Through the graphs (16-20) we observe that entropy generation attains maximum value near the walls of the tube and minimum value at the center of the tube.

It is observed from the graphs that entropy is directly proportional to ϵ, λ_1 ,M.

Figure (21-26) are representing the effects of parameters B_r, ϵ ,λ_1 ,M,Q,Λ on Beijan number (B_e).Through the graphs we can conclude that Beijan number (B_e) attains maximum vaue at the walls and minimum value in the interval $-0.5 \le r \le 0.5$.

5.Graphs

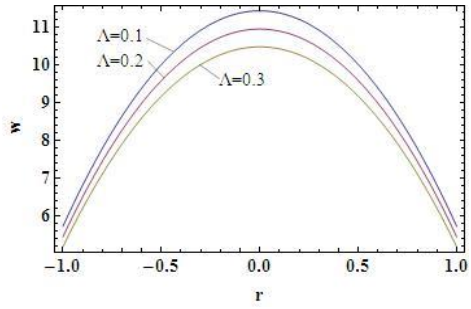

Fig 2: Velocity profile w (r,z) against the radial distance r for Λ

(z=1;$\epsilon = 0.1$; Q=0.1;M=1;$\lambda_1 = 0.02; \sqrt{D_a}$ =0.1; $\alpha = 0.01$)

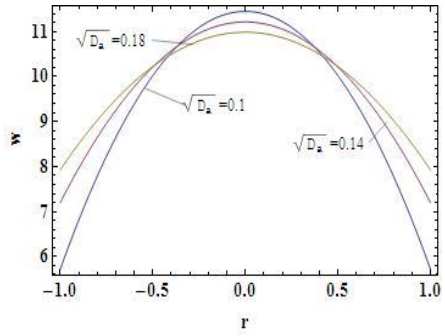

Fig 3: Velocity profile w (r,z) against the radial distance r for $\sqrt{D_a}$

(z=1;$\epsilon = 0.1$; Q=0.1;M=1; $\lambda_1 = 0.02; \Lambda = 0.1; \alpha = 0.01$)

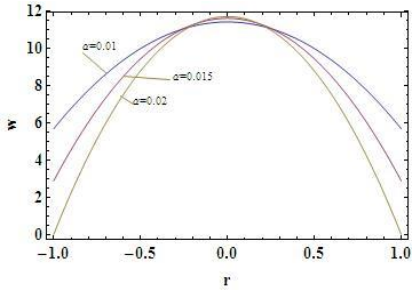

Fig 4: Velocity profile w (r,z) against the radial distance r for α

(z=1;$\epsilon = 0.1$; Q=0.1;M=1; $\lambda_1 = 0.02; \Lambda = 0.1; \sqrt{D_a} = 0.1$)

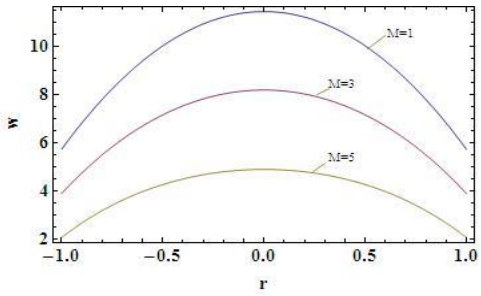

Fig 5: Velocity profile w (r,z) against the radial distance r for M

(z=1;$\epsilon = 0.1$; Q=0.1; $\alpha = 0.01; \lambda_1 = 0.02; \Lambda = 0.1; \sqrt{D_a} = 0.1$)

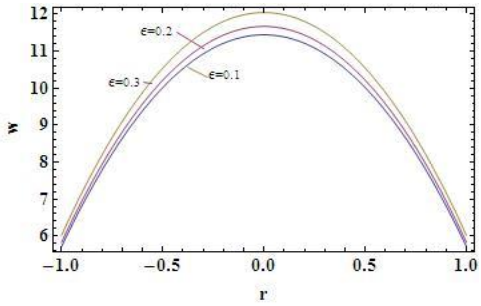

Fig 6: Velocity profile w (r,z) against the radial distance r for ϵ

(z=1; $\epsilon = 0.1$; Q=0.1;
$\alpha = 0.01; \lambda_1 = 0.02; \Lambda = 0.1; \sqrt{D_a} = 0.1$)

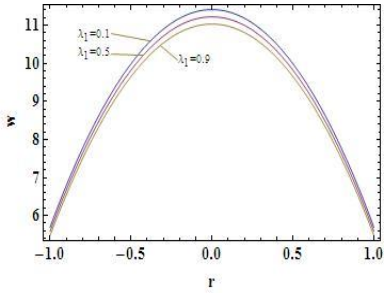

Fig 7: Velocity profile w (r,z) against the radial distance r for λ_1

($\epsilon = 0.1$; Q=0.1;M=1; α =0.01; $\Lambda = 0.1$;
$\sqrt{D_a} = 0.1$)

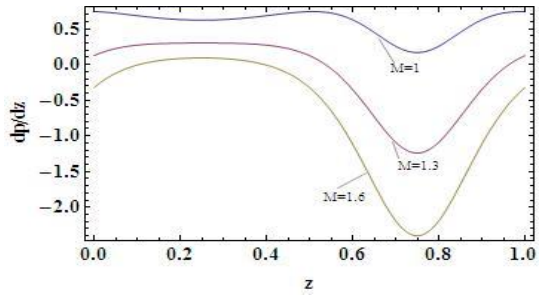

Fig 8: Pressure gradient dp/dz versus z for M

($\epsilon = 0.3$; Q=0.1;M=1; α =0.01
; $\lambda_1 = 0.1; \Lambda = 0.5; \beta = \frac{\sqrt{D_a}}{\alpha} = 0.1$)

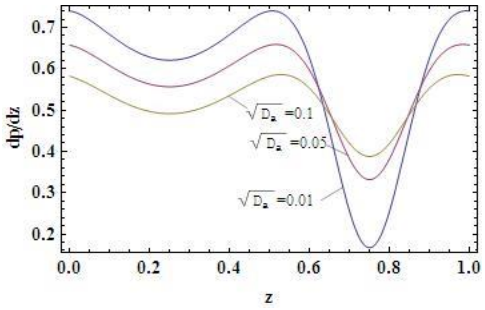

Fig 9: Pressure gradient dp/dz versus z for $\sqrt{D_a}$

($\epsilon = 0.3$; Q=0.1;M=1; α =0.1; $\lambda_1 = 0.1; \Lambda = 0.5$
)

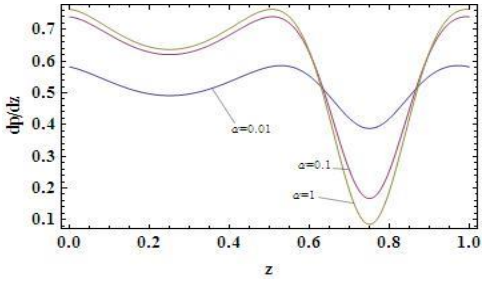

Fig 10: Pressure gradient dp/dz versus z for α

($\epsilon = 0.3$; Q=0.1;M=1; α =0.1
; $\lambda_1 = 0.1; \Lambda = 0.5; \sqrt{D_a}$ =0.01)

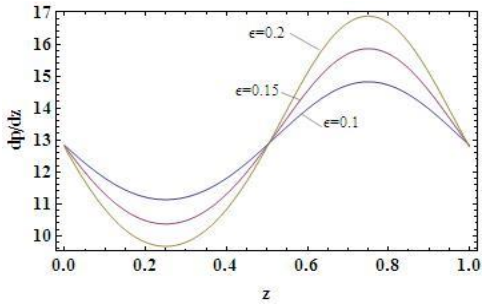

Fig 11: Pressure gradient dp/dz versus z for ϵ

($\epsilon = 0.3$; Q=0.1;M=1;
$\lambda_1 = 0.01; \Lambda = 0.1; \beta = \frac{\sqrt{D_a}}{\alpha} = 0.1$)

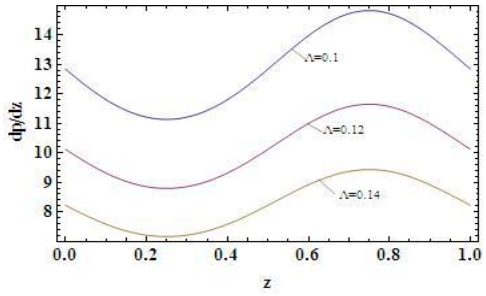

Fig 12: Pressure gradient dp/dz versus z for Λ

($\epsilon = 0.1$; Q=0.1;M=1;
$\lambda_1 = 0.01; \beta = \frac{\sqrt{D_a}}{\alpha} = 0.1$)

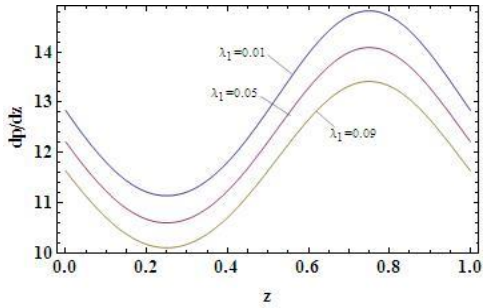

Fig 13: Pressure gradient dp/dz versus z for λ_1

($\epsilon = 0.1$; Q=0.1;M=1; $\Lambda = 0.1; \beta = \frac{\sqrt{D_a}}{\alpha} = 0.1$)

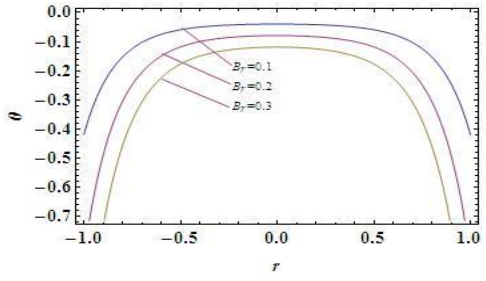

Fig 14: Temperature θ versus r for B_r

($\epsilon = 0.1$; Q=0.1; M=3;
$\Lambda = 0.5; \beta = 0.1; z = 0.1; \lambda_1 = 0.02; \gamma = 0.1$)

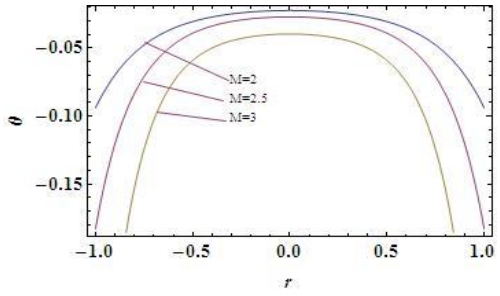

Fig 15: Temperature θ versus r for B_r

($\epsilon = 0.1$; Q=0.1; B_r =0.1;
$\Lambda = 0.5; \beta = 0.1; z = 0.1; \lambda_1 = 0.02; \gamma = 0.1$)

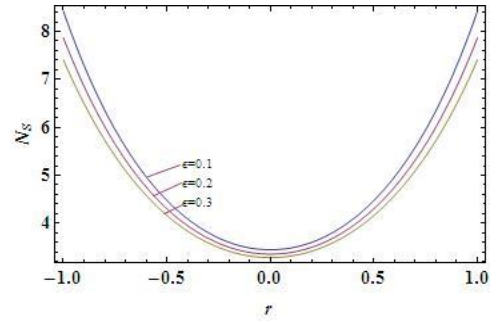

Fig 16: Entropy versus r for ϵ

(Q=0.1;M=1; B_r =0.1;
$z = 0.1; \Lambda = 0.1; \beta = 0.1; z = 0.1; \lambda_1 = 0.1; \gamma = 0.1; B_r = 1$)

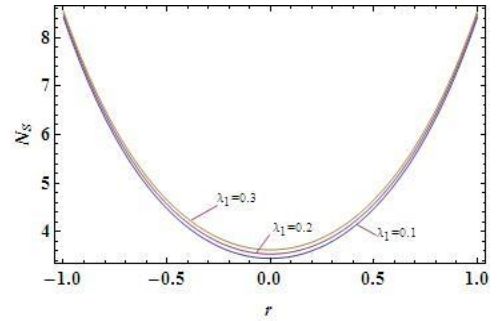

Fig 17:Entropy versus rfor λ_1

($\epsilon = 0.1$; Q=0.1;M=1; B_r =0.1;
$z = 0.1; \Lambda = 0.1; \beta = 0.1; \gamma = 0.1; B_r = 1$)

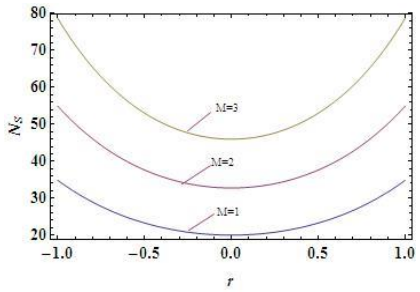

Fig 18: Entropy versus r for M

($\epsilon = 0.1$; Q=0.1; B_r =0.1;
$z = 0.1; \Lambda = 0.1; \beta = 0.1; \lambda_1 = 0.1; \gamma = 0.1; B_r = 1$)

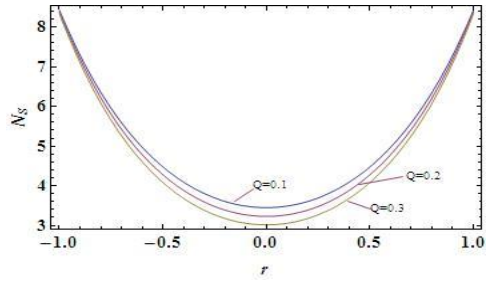

Fig 19: Entropy versus r for Q

($\epsilon = 0.1$; M=1; B_r =0.1;
$z = 0.1; \Lambda = 0.1; \beta = 0.1; \lambda_1 = 0.1; \gamma = 0.1; B_r = 1$)

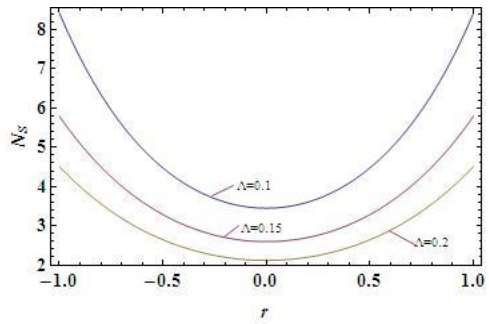

Fig 20: Entropy versus r for Q

($\epsilon = 0.1$; M=1; B_r =0.1;
$z = 0.1; Q = 0.1; \beta = 0.1; \lambda_1 = 0.1; \gamma = 0.1; B_r = 1$)

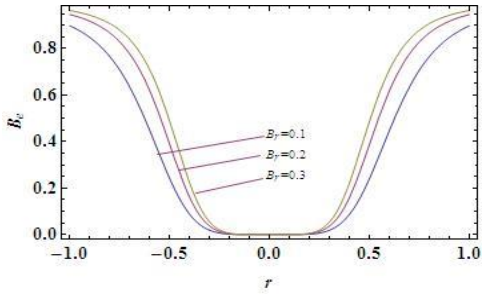

Fig 21: Variation of Bejan Numbers against the radial distances for B_r

($\epsilon = 0.1$; M=1; B_r =0.1;
$z = 0.1; \Lambda = 0.1; Q = 0.1; \beta = 0.1; \lambda_1 = 0.1; \gamma = 0.1$)

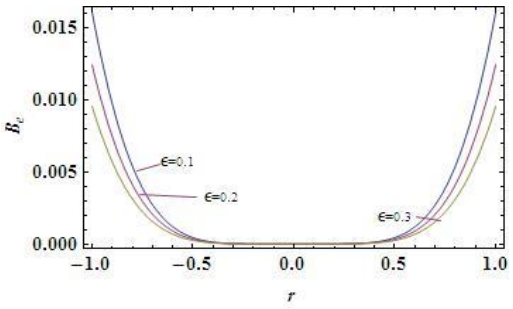

Fig 22: Bejan Numbers versus r for different ϵ

$[(B]_{\downarrow} r = 0.1$; M=1; B_r =0.1;
$\Lambda = 0.1;\ z = 0.1; Q = 0.1; \beta = 0.1; \lambda_1 = 0.1; \gamma = 0.1$
)

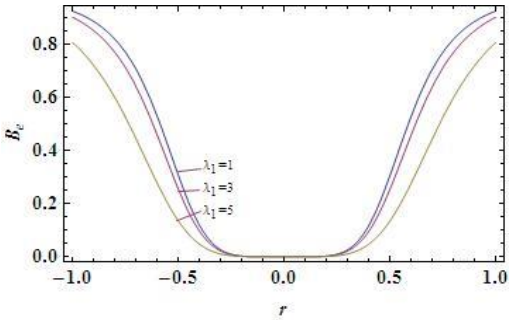

Fig 23: Bejan Numbers versus r for different λ_1

($B_r = 0.1$; M=1; $\Lambda = 0.1$; B_r =0.1;
$z = 0.1; Q = 0.1; \epsilon = 0.1; \gamma = 0.1$)

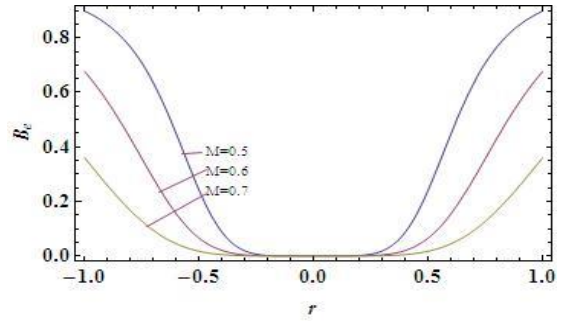

Fig 24: Bejan Numbers versus r for different M

$$\left[\!\left[(B \right]\!\right]_{\downarrow} r = 0.1 \; ;$$
$$\Lambda = 0.1;\; z = 0.1; Q = 0.1; \epsilon = 0.1; \lambda_1 = 0.1; \gamma = 0.1$$
)

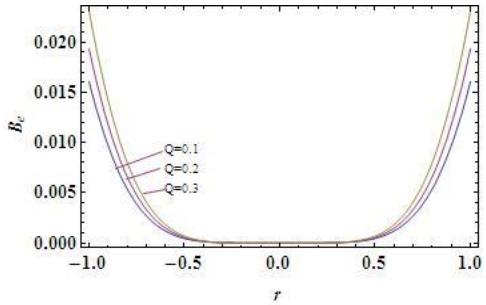

Fig 25: Variation of Bejan Numbers against the radial distances for Q

($B_r = 0.1$;
$\Lambda = 0.1; z = 0.1; M = 1; \epsilon = 0.1; \lambda_1 = 0.1; \gamma = 0.1$
)

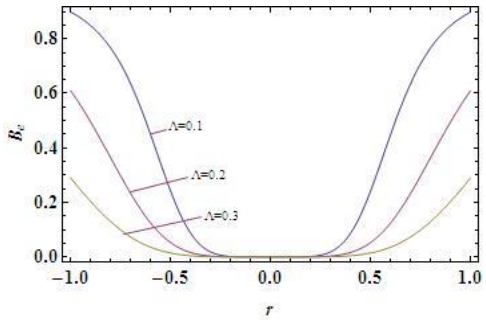

Fig 26: Variation of Bejan Numbers against the radial distances for Λ

($B_r = 0.1$; M=1;
$z = 0.1; Q = 0.1; \epsilon = 0.1; \lambda_1 = 0.1; \gamma = 0.1$)

6. CONCLUSION

The Present work addresses the Entropy generation analysis of peristaltic flow of jeffery nanofluid in a tube with permeable walls.the following observations are made Velocity profile(w) and temperature profile(θ) are attaining maximum value at the center and minimum value at the walls of the tube. Entropy generation(NS) attains maximum value near the walls of the tube and minimum value at the center of the tube.

REFERENCES

[1] 1.Latham.W.(1966):Fluid motion in a peristaltic pump.Master's Thesis,MIT,Cambridge,MA,USA.
[2] 2.Shapiro,A.H.(1967):Pumping and retrograde diffusion in peristaltic waves.In proceedings of the Workshop in Ureteral Reflux in children,Washington,DC,USA,11-12 November volume 1,pp.109-126.
[3] 3.Srinivas,S;kothandapan,M.;(2008):Peristaltic transport in an asymmetric channel with heat transfer –A note Int commun.Heat mass transfer,35,514-522.
[4] 4.Akber,NS;.Nadeem,S.;Hayat,T.; Obaidat,S.;, (2012):Int.J.Heat Mass transfer 55,1855.
[5] 5.Mekheimer,K.S;Elamaboud,A.;Abdellateef,A.I .; (2013):Particulate suspension flow inducew induced by sinusoidal peristaltic waves through eccentric cylinders;Thread annular.Int.J.Biomath .
[6] 6.Girija Devi,R;Devanathan. (1975):Peristaltic motion of a micropolar fluid;Proceedings of Indian Academy of Sciences-section A 81(4),149-163.
[7] 7.Muthu, P.;Rathish, B.;,Candra,V.; (2008):Peristaltic motiopolar on of micropolar fluid in circular cylindrical tubes;Effect of wall properties[J].Applied Mathematical modeling,32(10):2019-2033.
[8] 8.Choi, S.U.S. (1995):Enhancing thermal conductivity of the fluids with nanoparticles.ASME Fluids Eng.Div. 231,99-105.
[9] 9.Akber ,N.S. (2014):Peristaltic flow with Maxwell carbon nanotubes suspensions[J]Journal of computational and theoretical nanoscience,11(7):1641-1648.
[10] 10. Akber ,N.S.(2014): Endoscopic effects on the Peristaltic flow of cu-water nanofluid[J] Journal of computational and theoretical nanoscience,11(14):1150-1155.

[11] 11Abbasi,F.M.;Hayat,T.;Ahmad,B.;Chen,G.Q.; (2014):Peristaltic motion of non Newtonian nanofluid in an asymmetric channel.Z,Naturforsch,69,451-461.
[12] 12. Akber, N.S.;Nadeem ,S.; (2013):Studied the mixed convective Peristaltic motion of MHD Jeffrey nanofluid in an asymmetric channel with Newtonian heating. Z,Naturforsch.68a,4.68a,433-441.
[13] 1.Narla,V.K.;Ramanamurthy,JV.; (2015): Peristaltic transport of Jeffrey nanofluid in curved channels.Proeng 11.424.
[14] 14.Jie Li ,Clement Kleinstreuer ,Entropy generation analysis for nanofluid flow in Microchannel. Journal of Heat transfer V 132(12)
[15] 15Souidi,F.;Ayachi,K.;Benyahia,N.;(2009): Entropy generation rate for a peristaltic pump .Journal of Non equilibrium.
[16] 16Hayat,T.;Saleem Asgha,(2017): Entropy generation analysis for Peristaltic flow of nanoparticles in a rotating frame .10.1016/j.ijheatmasstransfeR
[17] 17. Akber, N.S.;Adil Wahid Butt,(2017): Entropy generation analysis for Peristaltic flow of cu-water nano fluid in a tube with viscous dissipation,Journal of Hydrodynamics. 29(1);135-143.
[18] 18.Abu-Nada, E. (2006):Entropy generation due to heat and fluid flow in backward facing step flow with various expansion ratios [j].international journal of exergy,3(4):419-435.
[19] 19 Abu-Nada, E.(2005):Numerical prediction of Entropy generation in seerated flows[j],7(4):234-252.
[20] 20.Hijleh, B.A.;Abu-Qudais, M.; Abu-Nada, E.;(1999):.Numerical prediction of entropy generation due to natural convectio from a horizontal cylinder [j],ENERGY,24(4):327-333.